

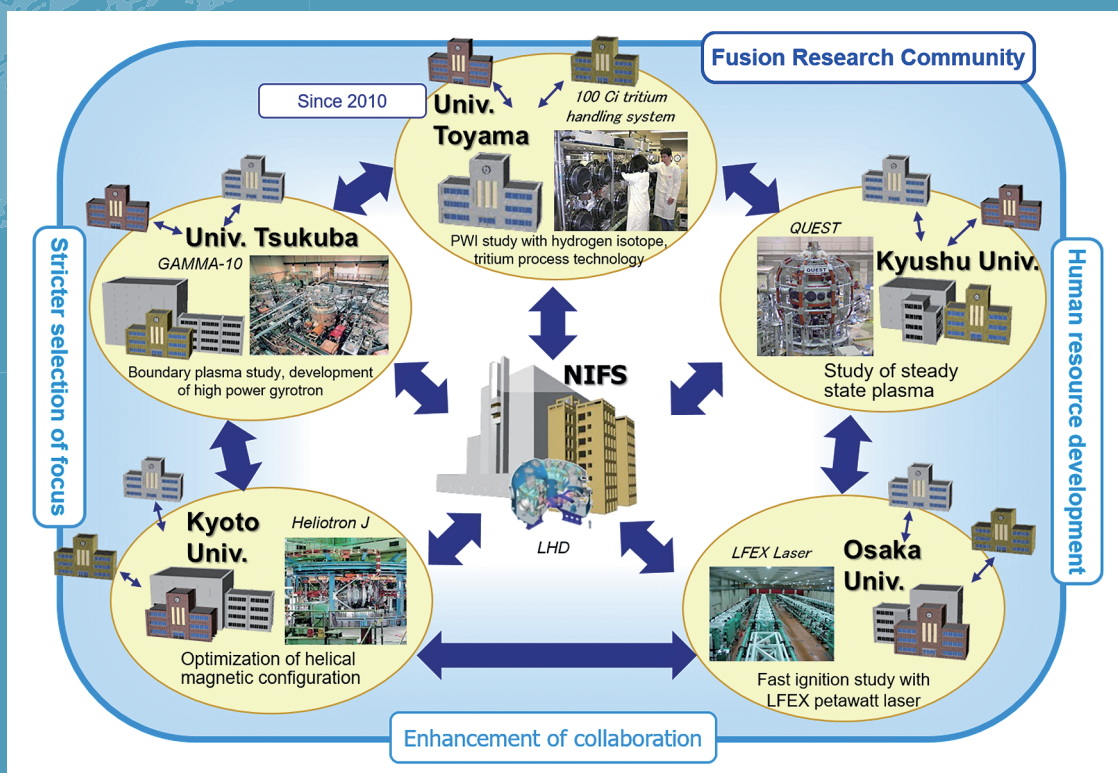
# 8. Bilateral Collaboration Research Program

The purpose of the Bilateral Collaboration Research Program (BCRP) is to enforce the activities of nuclear fusion research in the universities by using their middle-size experimental facilities of the specific university research centers as the joint-use facilities for all university researchers in Japan. The current program involves 5 university research centers, as follows:

- Plasma Research Center, University of Tsukuba
- Laboratory of Complex Energy Process, Institute of Advanced Energy, Kyoto University
- Institute of Laser Engineering, Osaka University
- Advanced Fusion Research Center, Research Institute for Applied Mechanics, Kyushu University
- Hydrogen Isotope Research Center, University of Toyama

In BCRP, each research center can have its own collaboration programs using its main facility. Researchers at other universities can visit the research center and carry out their own collaboration research there, as if the facility belongs to NIFS. That is, all these activities are supported financially by NIFS as the research subjects in BCRP. The BCRP subjects are subscribed from all over Japan every year as one of the three frameworks of the NIFS collaboration program. The collaboration research committee, which is organized under the administrative board of NIFS, examines and selects the subjects.

(T. Morisaki)



## Study of boundary plasmas by making use of open magnetic field configuration and development in high power gyrotrons towards the DEMO project

In the Plasma Research Center, University of Tsukuba, studies of boundary plasma and development of high-power gyrotrons have been performed under the bilateral collaboration research program. GAMMA 10/PDX is the world's largest tandem mirror device and has many plasma production/heating devices with the same scale of present-day fusion devices. In FY2018, 24 subjects including the base subject were accepted and were productive of a number of excellent results.

Numerous divertor simulation experiments at the end region have been carried out with strong ICRF and ECH systems. Figure 1 shows a schematic view of GAMMA 10/PDX and a divertor simulation experimental module (D-module) that is installed at the west end region. The D-module consists of a rectangular box (0.5 m square and 0.7 m in length) with an inlet aperture at the front panel and a V-shaped target system inside the box. Plasma facing material of the V-shaped target is tungsten. The target size is 0.3 m in width and 0.35 m in length. The end loss plasma is exposed to the target. Additional hydrogen gas and several kinds of radiator gasses (N<sub>2</sub>, Ne, Ar, Kr, and Xe) can be supplied into the D-module.

When the neutral pressure in the D-module was increased higher than 12 Pa by the additional hydrogen gas supply, Balmer line emissions from highly excited hydrogen atoms ( $n \geq 5$ ) significantly increased. In addition, a population inversion with  $n_H (n=5)$  larger than  $n_H (n=4)$  was observed although  $T_{vib}$  became rather low (~2,000 K). Detailed analysis revealed the production of the highly excited hydrogen atoms, and the population inversion are attributed to the reaction of mutual neutralization between molecular ions and negative ions. The negative ions are considered to be produced by the resonant ionization process between H(2s).

In the radiator gas injection experiments for detached plasma formation, additional heating pulses of ECH were applied in the upstream region and the effect of plasma heating on the detached plasma was investigated.

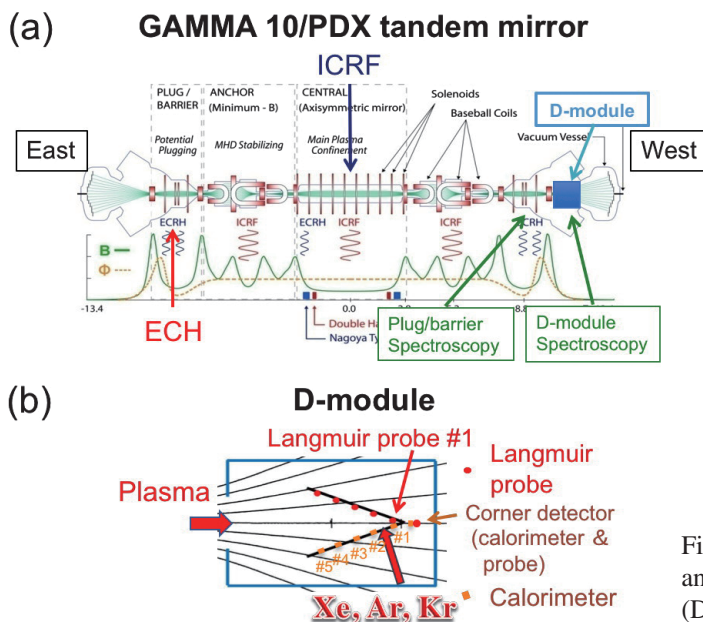


Fig. 1 Schematic view of GAMMA 10/PDX and divertor simulation experimental module (D-module).

Figure 2 shows dependence of heat flux at the corner of the V-shaped target on the Xe plenum pressure  $P_{Xe}$  in the cases of with and without the additional ECH. When the Xe gas was not supplied (i.e.,  $P_{Xe} = 0$ ), the heat flux was increased by about twice due to ECH. On the other hand, the heat flux was increased by more than 10 times due to ECH when the Xe gas was supplied, and the heat flux decreased with increase in the Xe plenum pressure. It is found that ion flux and heat flux are abruptly increased during ECH and the detached to attached transition occurs. Moreover, combination of hydrogen gas and a small amount of nitrogen gas causes significant decrease in plasma density and ion flux to the target, indicating importance of a recombination process (N-MAR) related to nitrogen gas.

Figure 3 shows a schematic view of the Thomson scattering system at the west end region. The electron density and temperature at the D-module could be measured for the first time due to reduction of stray light. Further, the multi-pass Thomson scattering system was improved to double the number of passes through installation of a laser amplification system.

In ICRF heating studies, the following subjects were studied: the effect of end-loss ion flux on increase in plasma density and potential at the central cell due to ICRF heating, and spatial structures of AIC (Alfvén-ion-cyclotron) waves and difference frequency waves at the central cell and energy distribution of high energy ions which flowed out to the end region by interaction with the above mentioned waves.

In the 2018 experimental test of a new 28/35 GHz dual-frequency gyrotron (2 MW for 3 s and 0.4 MW CW) for QUEST, NSTX-U, Heliotron J, and GAMMA 10/PDX, maximum powers of 1.65 MW at 28.04 GHz and 1.21 MW at 34.83 GHz were achieved by improving the power supply. A detailed design for a 14 GHz 1 MW gyrotron is advancing toward its fabrication. For a 14 GHz radio frequency (RF) beam with high divergence, a calculated transmission efficiency of 94% to the corrugated waveguide coupling position was obtained by introducing the design concept (direct RF beam coupling by built-in waveguide) to minimize the RF transmission path. Installing a double-disk sapphire window will make it possible to develop a 1 MW gyrotron with a continuous wave (CW) at 14 GHz.

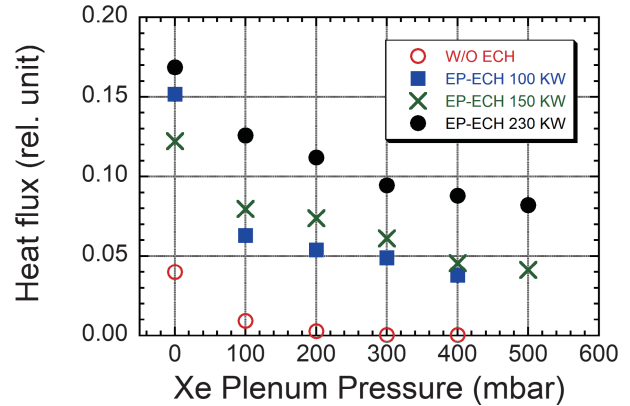


Fig. 2 Dependence of heat flux at the corner of the V-shaped target on the Xe plenum pressure  $P_{Xe}$  in the cases of with and without the additional ECH.

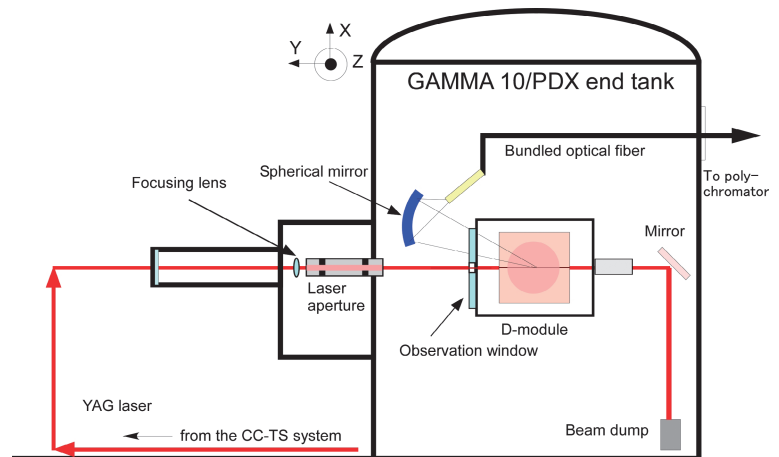


Fig. 3 Schematic view of the Thomson scattering system at the west end region.

(M. Sakamoto)

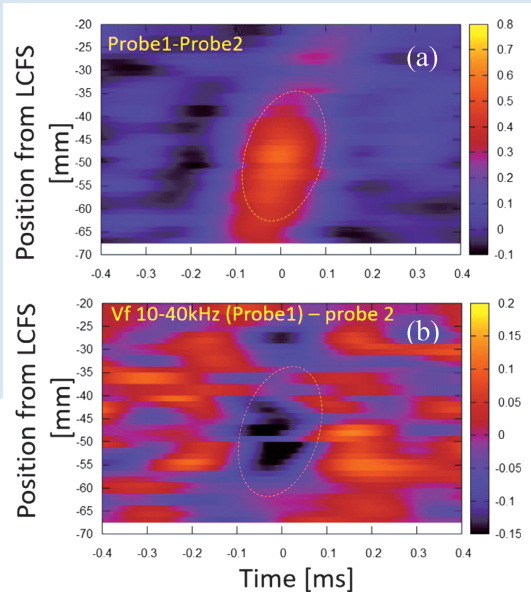


Fig. 1 Zonal flow (ZF) measurement: (a) spatio-temporal structure of ZF obtained with correlation analysis between different probe signals, and (b) correlation between ZF and turbulence amplitude in the frequency range of 10–40 kHz [1].

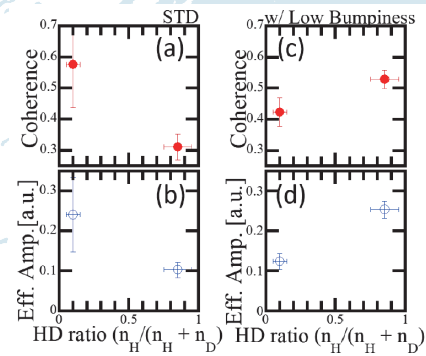


Fig. 2 Isotope dependence of coherence ((a)&(c)) and effective amplitude ((b)&(d)) in the frequency component (<4 kHz) corresponding to zonal flow in standard and low-bumpiness configurations.

Highlight

## The configuration dependence of isotope effects on turbulence system in Heliotron J

The hydrogen/deuterium (H/D) isotope effect on fluctuations and its configuration dependence are studied in Heliotron J. The isotope dependence of a toroidally symmetric fluctuation in a low frequency range of  $< \sim 4$  kHz, which is considered as a zonal flow, is observed in low-density ECH plasmas. A zonal flow is considered relating to transport physics in plasmas, such as steady-state transport, L-H transition, limit cycle oscillation, avalanche and isotope effects on confinement properties. Main diagnostics in this experiment are multiple Langmuir probes installed at different toroidal/poloidal sections, which are separated by  $67.5^\circ$  in toroidal angle. In order to extract a structure of zonal flow, an effective zonal flow amplitude was evaluated, based on the technique using the total amplitude and coherence in the zonal flow frequency range. Figure 1 shows that the turbulence suppression is observed only at  $\sim 50$  mm where the zonal flow amplitude has a maximum. Figure 2 shows the dependence of the coherence less than 4 kHz and the effective amplitude on H/D ratio by fuel gas change. The fraction of D is more than  $\sim 80\%$  in the D discharges, and less than  $\sim 15\%$  in the H discharge. Two columns of figures show the comparison between the standard (medium-bumpiness) configuration and low-bumpiness configuration in Heliotron J. The results exhibit that both coherence and effective amplitude of ZF decrease in D plasmas, differently from the standard configuration and Tokamaks, but similarly to the observation in a helical machine, TJ-II. The fact simply suggests that the isotope effects on turbulence system should be dependent on the magnetic configurations. The fluctuation with long-range toroidal correlation becomes stronger and the correlation is enhanced in D dominant plasmas in standard configuration of Heliotron J, which shows that the confinement of turbulence transport should be improved in D plasmas. Interestingly, however, the opposite dependence on isotope ratio is observed in the magnetic configuration tagged here “low-bumpiness”.

[1] S. Ohshima *et al.*, “The Configuration Dependence of Isotope Effects on Turbulence System in Heliotron J”, 27th IAEA Fusion Energy Conference (FEC2018), 22–27 Oct. 2018, Gandhinagar, India, EX/P3-3.



## Research Topics from Bilateral Collaboration Program in Heliotron J

The common objectives of the researches in Heliotron J under this Bilateral Collaboration Program are to investigate experimentally/theoretically the transport and stability of fusion plasma in advanced helical-field, and to improve the plasma performance through advanced helical-field control. Picked up in FY2018 are the following seven key topics; (1) studies of plasma transport and related plasma self-organization through advanced helical magnetic field control, (2) study of electron cyclotron heating (ECH)/current drive (ECCD) heating mechanism and its improvement, (3) production of high density NBI plasmas and confinement study of high-beta plasmas, (4) boundary plasma study in an advanced helical device, (5) study of instability control, (6) experimental study of plasma current by field configuration control in an advanced helical device, and (7) empirical research of new experimental methods and analysis methods. Two key topics are described below.

**Effect of magnetic field structure on electron internal transport barrier (eITB) and its role for the transport barrier formation:** The internal transport barrier has been observed widely in helical devices such as CHS, LHD, TJ-II, W7-AS, and Heliotron J. During eITB, effective heat transport in the plasma core region is reduced in low density ECH plasmas in Heliotron J. The effect of the ripple on the eITB formation was investigated by changing bumpiness of the magnetic configuration. The central electron temperature of the ECH plasma as a function of the injected power divided by the line averaged density in low density region ( $\bar{n}_e < 1 \times 10^{19} \text{ m}^{-3}$ ) depends on the bumpiness. The power thresholds to form the eITB in the low and the high bumpiness configurations are larger ( $550 \times 10^{-19} \text{ kWm}^3$ ) than that of the medium bumpiness ( $250 \times 10^{-19} \text{ kWm}^3$ ). Consequently, the smaller  $\epsilon_{eff}$  configuration has the lower power threshold in Heliotron J, and this result does not agree with the CHS results. It is possible that the rational surface or the magnetic island affects the eITB formation in Heliotron J result. For the investigation of rational surface effect, current ramp-up experiment is performed near the threshold heating power of the formation of eITB. The bootstrap current gradually increases during the discharge, the central value of  $T_e$  increases at the plasma current of near 0.9 kA. At this timing, the central temperature increased and the eITB expands outwardly with a fast time scale compared to the energy confinement time. The 4/7 low-order rational surface is expected to be created by the current ramp up. This eITB is caused by the rational surface formation inside plasma.

**Control of fast-particle-driven MHD instability by using ECH/ECCD:** Fast-particle (FP)-driven magnetohydrodynamics (MHD) instabilities enhance anomalous transport and/or induce the loss of fast particle including alpha particles in a D-T fusion reactor. Since redistribution and exhaust of alpha particles lead to reduction of fusion gain  $Q$  and damage of first wall, to establish methods of stabilization and/or control of FP-driven MHD instabilities is required for the D-T fusion reactor, but they have not been established yet. ECH/ECCD are a candidate method to control the FP driven MHD instabilities because ECH/ECCD may be an ideal tool to control the modes since they can provide highly localized EC waves with a known location and good controllability of heating position and parallel refractive index  $N_{||}$ . Both negative and positive magnetic shear, which is induced by co- and counter-EC-driven plasma current, suppress the observed energetic particle modes (EPMs) with  $m/n = 2/1$ . EPM amplitude has a maximum around plasma current of  $I_p = 0.2 \text{ kA}$  and decreases with the increase of the plasma current regardless of sign of plasma current. The absolute value of rotational transform is considered to contribute to this mode suppression. The global Alfvén eigenmodes (GAEs) with  $m/n = 4/2$  has the same tendency. Such suppression effect of FP-driven MHD instabilities is also observed in other helical devices, LHD and TJ-II. ECCD stabilization seems to be a common effect for helical devices.

(K. Nagasaki, H. Okada, S. Ohshima, T. Minami, S. Yamamoto, S. Kado and S. Kobayashi)

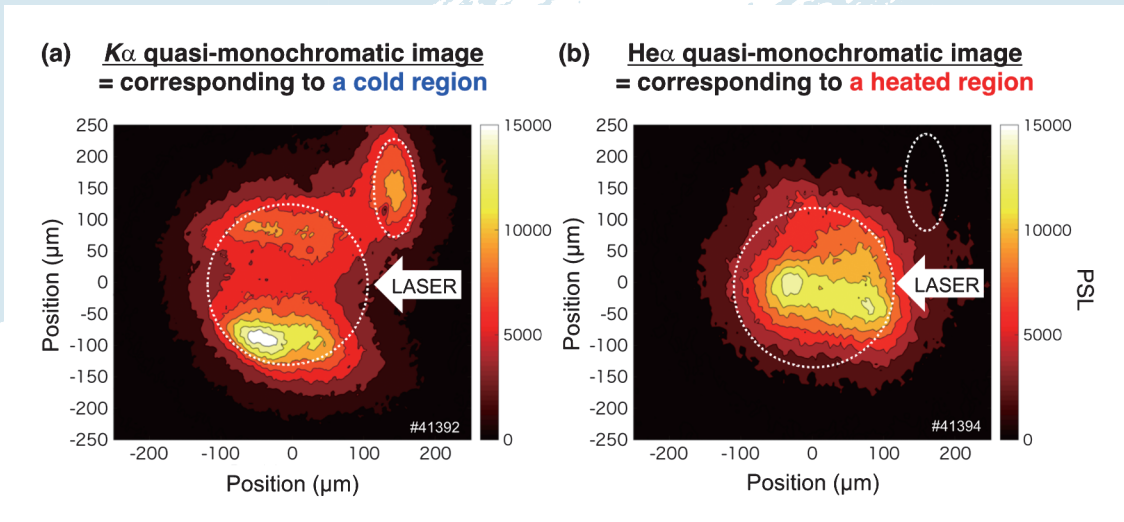


Fig. 1 X-ray emission images of (a) K-alpha lines and (b) He-like lines from doped Ti ions.

Highlight

## Heating performance of Fast Ignition target by intense short-pulse irradiation

We have developed a Fresnel zone plate imager spectrally tuned to specific x-ray line emissions from the dopant element (Ti) in the compressed plasma which enables us to obtain monochromatic images to visualize the plasma states with a high spatial resolution. Figure 1 (a) shows an image of K-alpha x-ray emissions from the imploded plasma, which corresponds to the relatively cold region of the plasma in which the dopant (Ti) was not highly ionized and can emit K-alpha lines via collisions of hot electrons. On the contrary, Fig. 1 (b) shows an image of He-alpha lines of Ti, which means the Ti ions were heated and ionized to He-like state there. These images clearly indicate that the heating was performed at around the central axis of the imploded plasma by fast heating, and the regions surrounding the axis were kept relatively cold.

## Fast Ignition of Super High-Dense Plasmas

Laser-driven inertial confinement fusion by the Fast Ignition (FI) scheme has been intensively studied as the FIREX-1 project at the Institute of Laser Engineering, Osaka University. The researches consist of target fabrication, laser development, fundamental and integrated implosion experiments, simulation technology and reactor target design, and reactor technology development. In FY2018, the following progress was made through the Bilateral Collaboration Research Program with NIFS and other collaborators from universities and institutes (NIFS12KUGK057 as the base project and 17 individual programs).

### Theory and Simulation, Target Design

It has been demonstrated so far that the imploded plasma was heated up to 1.7 keV with a heating efficiency up to 8%. In FY2018, we have investigated the physical mechanisms there by using a PIC simulation code named “PICLS” which includes atomic processes such as collisions, ionizations, and so forth. It was found that the thermal diffusion from the directly laser-heated region to the neighboring areas in the imploded plasma is performing an important role in the total plasma heating as shown in Figure 2. Also found is that a kilo-Tesla class magnetic field was generated by resistive current and was guiding the fast electron flow together with the externally applied magnetic field. We studied the heating efficiency taking into account such physical mechanisms to establish a scaling law of the heating.

By taking into account those findings, heating of the fuel plasma with a density of 100 g/cc by a 10 kJ/10 ps class laser was evaluated in order to design 5 keV heating.

### Target Fabrication and Reactor Technology

Refractive index of liquid/solid DT mixture is of great importance in inertial fusion research since the fuel pellet is expected to be inspected by using optical diagnostics. We performed an experiment to create solid-state  $D_2$  and  $T_2$  mixture, and successfully measured its refractive index, which was found to be close to the expected value inferred from the similarity with  $D_2$  and  $H_2$ . It also was found that the spatial distributions of  $D_2$  and  $T_2$  are slightly different with each other, which is attributed to the heat generation due to beta-decay of T.

### Operation and improvement of GEKKO-XII/LFEX Laser system

Isentropic implosion is essential for controlling the shock wave velocity from each part of the fuel layer. Advanced pulse shape control technology was developed for GEKKO-XII laser oscillator system. A simulation code was developed taking into account amplifier performance as well as frequency conversion parameters in KDP crystals. Figure 3 (a) shows typical results of 4-ns flat-top pulse shape for three beams, all in a sufficiently good agreement. Three-step pulse shape is one of the candidates for high-density implosion. Blue line in Fig. 3 (b) is the designed shape, and black line is a typical result. Although the 1st and the 2nd steps (flat-top) were well controlled, the peak power of the 3rd pulse was still lower than expected. Further improvement will be continued in FY 2019.

### Individual Collaborations

In parallel with the main project described above, 17 other collaborations by individual researchers including two from abroad have been performed. Those projects were on electron-driven fast ignition (8 collaborations), ion-driven fast ignition (2), alternative scheme of laser-driven inertial fusion (2), diagnostics of high-temperature and high-density plasmas (4), and reactor technology (2). 9 were projects continued from the previous year(s) and 8 were newly accepted in FY2018.

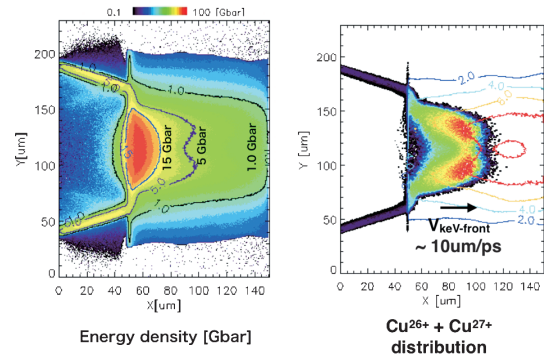


Fig. 2 Simulation results of magnetically assisted fast ignition. (a) Electron pressure distribution after the heating by LFEX laser. (b) Spatial distribution of 26th and 27th ionized Cu dopants which correspond to the heated region.

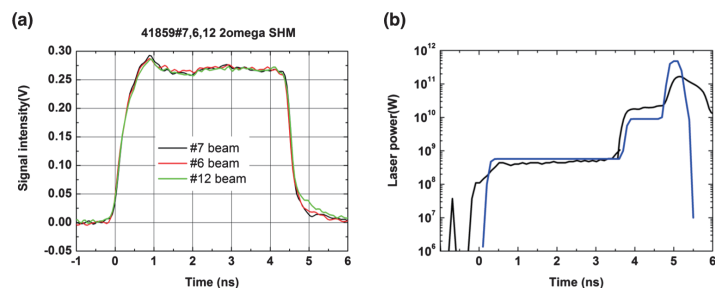


Fig. 3 (a) Flat-top pulse shapes of three beams. (b) A three-step pulse, designed (blue line) and achieved (black).

(R. Kodama, H. Shiraga, S. Fujioka, Y. Sentoku, K. Yamanoi and Y. Arikawa)

### Research activities on QUEST in FY2018

We will summarize the activities on advanced fusion research center, research institute for applied mechanics in Kyushu University during April 2017 – March 2018. The QUEST experiments were executed during 12th May – 5th Aug. (2017 Spring/Summer; shotno 34700–35819) and 30th Nov. – 9th Mar. (2017 Autumn/Winter; shotno 35820-36662). Main topics of the QUEST experiments in FY2018 are listed below.

- 1) The highest plasma current discharge of 93kA in non-inductive current drive adding a bit of ohmic heating was obtained by 28 GHz microwave injection which developed with Tsukuba University (Gyrotron) and NIFS (polarizer) (shotno 35682). The control of refractive index parallel to the magnetic field,  $N_{\parallel}$  could give us the controllability of branching in electron energy selectivity during plasma start-up without fundamental ECH.
- 2) The neutral compression behind the lower divertor plates with downward ion toroidal drift and up-down asymmetry of the hot wall temperature during more than an 1h discharge. (The lower hot wall temperature was higher than upper one.) The compression was observed after approximately 2000 sec from the plasma initiation, and then a bright area measured with a visible video-camera came up around the center stack beside the lower divertor plate. This suggests that fuel neutral got collected at the lower natural divertor area, although the reason is still unclear.
- 3) The densities measured by the Thomson scattering system were calibrated using a newly fabricated microwave interferometer with the probing frequency of 50 GHz. We obtained the density and temperature profiles of the plasmas sustained by 8.2 GHz ECH. For the case of inboard poloidal field null configuration, the maximum electron temperature was about 300 eV (at the inboard side) and the density was about  $2 \times 10^{17} \text{ m}^{-3}$ .
- 4) Recovery of the previous permeation probes that were installed in QUEST several years ago was conducted for the measurement of hydrogen atomic flux at the wall. Functionality of the devices has been confirmed successfully as detection of signal from a quadrupole mass analyzer, for 4 probes out of 5 installed.
- 5) The plasma shape reconstruction by the Cauchy condition surface method with the Mirnov type magnetic sensors, which have very large coupling area and were made for JT-60SA, and ex-vessel hall sensors is being prepared for QUEST.
- 6) In order to improve the high plasma current divertor operation, to help the transition from CHI discharge to Ohmic discharge, and to provide the vertically unstable negative triangular plasma, the feedback control system for the plasma vertical movement is required in the present QUEST. To design this control system, the plasma circuit equations with the vacuum chamber currents with 30 loops, the horizontal field coil and the plasma vertical movement should be solved numerically. In 2018, the basic research has been started how to tackle this problem and the research target has been clarified to go forward.
- 7) Considering the toroidal rotation, the equilibrium is fitted within nested magnetic surfaces by SU-EFIT. Sweeping the ratio of the current density due to the toroidal rotation and the one due to the pressure gradient, the relation between the peak toroidal rotation speed squared and the poloidal beta value is linear. Namely, sum of contributions from toroidal rotation and pressure gradient to plasma current density is constant.
- 8) The W sample was placed on the plasma facing wall in QUEST and exposed to hydrogen plasma during 2017 SS, 2017 AW or 2018 SS campaign. Additional D2 + implantation and then TDS experiments were performed. It was found that a lot of damages were introduced for the short-discharge 2017 sample, and D was also retained by these damages. But, for 2018SS, D retention was clearly reduced and only lower D desorption at low temperature was found, suggesting that the irradiation damages do not depend on the discharge time but the plasma current.
- 9) A comparative measurement of the ion toroidal velocity was conducted at the midplane in 28 GHz and 8.2 GHz IL and IPN discharges using optical emission spectroscopy. A particularly large velocity of up to 4 km/s (Mach number  $\sim 1$ ) was found in the outer SOL of IPN discharge.
- 10) Thermal desorption of hydrogen from atmospheric plasma spray tungsten (APS-W) layers, plasma-facing material of QUEST, was examined after exposure to QUEST plasma. The release of hydrogen from APS-W started at around 100°C and peaked at around 400°C. This observation suggests significant reemission of hydrogen from APS-W at wall temperature of QUEST.
- 11) A multi-aperture grid of the low energy ion source (10 keV) was designed to produce high current ion beams for the QUEST NBI. 14.9 A ion beams are extracted from a 30 cm diameter area with 1180 numbers of



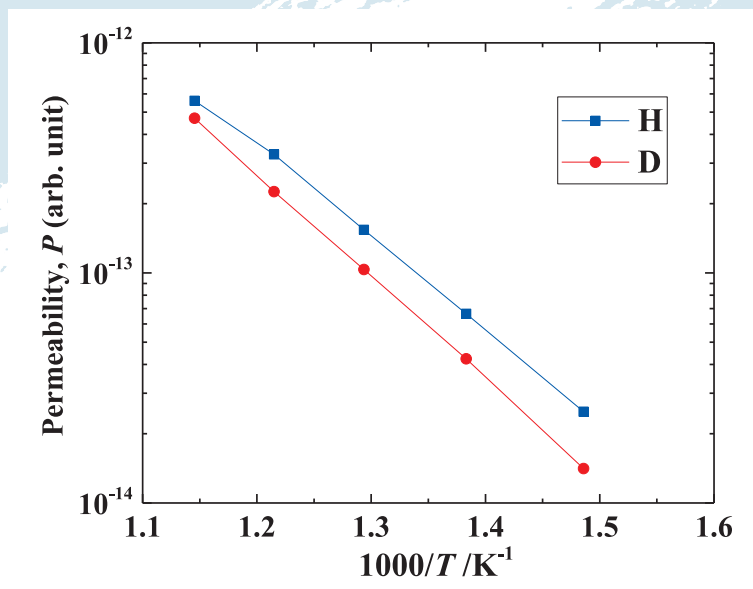
- apertures and cooling channels at 100 mA/cm<sup>2</sup> ion current density. It enables 101 kW injection power. Focusing of beams to the injection port were analyzed with 3D beam trajectory simulation. 0.42 mm displacement of the extraction grid aperture axis deflects the ion beam by 36 mrad for focusing.
- 12) Overall control system of QUEST has been modified continuously according to the progress of recent technology. As an example, an administration system for entry experimental hall has been developed, which is composed of pocket-size PC with Wi-Fi and touch panel display. This system is contributory to the secure operation of QUEST with shutting down the sequence safely when someone stays in experimental hall.
  - 13) A new drift tube, inside of which is a CT guiding tube made of OFC-Cu for conservation of CT magnetic flux, has been installed on the CT injector. The replacement of the drift tube leads to improve CT fueling efficiency. The injector has been detached from QUEST and set up for wall-conditioning and test operation.
  - 14) Hybrid probe, which consist of the magnetic probes and Langmuir probes, was installed in QUEST to get the electro-magnetic signal associated with peripheral plasma fluctuation. This time it is confirmed the probe function by using 28 GHz ECH injection experiment.
  - 15) Temperature dependence of tritium retention in tungsten under irradiation of tritium ions has been examined using  $\beta$ -ray induced X-ray spectrometry. Retention of tritium in surface layers decreased with temperature rise, while it contrarily increased above 523 K, and it was suggested that change in the tritium retention strongly depends on solubility of tritium in surface layers in comparison with effect of diffusion into the bulk of tungsten.
  - 16) Electron cyclotron non-inductive plasma start-up of an 90 kA level has been achieved with an obliquely injection of a polarized 28 GHz focusing-beam. The incident-wave polarization was carefully controlled to obtain significant single pass absorption. Bulk-electron heating was attained in a perpendicular injection. Relatively high electron temperature of 200 eV was attained in a plasma with density of  $5 \times 10^{18} \text{ m}^{-3}$  and current of 25 kA.
  - 17) The paper “Initial results from solenoid-free plasma start-up using Transient CHI on QUEST,” by K. Kuroda *et al.*, was published in *Plasma Physics and Controlled Fusion* 60 (2018) 115001. The paper describes the generation of 45 kA of toroidal current from the operation of a new reactor-relevant transient CHI electrode configuration that should be easier for implementation in reactor configurations. In a supporting paper, “TSC Simulation of Transient CHI in New Electrode Configuration on QUEST”, by K. Kuroda *et al.*, published in the journal *Plasma and Fusion Research*, 13, (2018) 3402058, the numerical simulation results aimed at improving the CHI experimental performance on QUEST is described.
  - 18) A new series of Chubu-Kyushu Univ. joint experiments have been conducted to investigate the effect of forced convection on the heat transport in liquid metals, using a modified TDS setup brought from NIFS in the last fiscal year. Results indicate that the heat transport is significantly enhanced by liquid convection induced by the  $\mathbf{J} \times \mathbf{B}$ -electromagnetic force.
  - 19) In tokamak plasmas produced by 28 GHz ECH launching, divertor biasing experiment was carried out, aimed at two purposes: (1) to drive SOL current for generating resonant magnetic perturbations (RMP), and (2) to broaden divertor heat load. The experimental data show a potentiality of the divertor biasing.
  - 20) Electron Bernstein wave (EBW) heating/current drive is one of the key issues to attain steady state tokamak configuration in the QUEST. The collective scattering system utilizing the 400 GHz gyrotron and quasi-optical transmission/antenna/reflector gratings are designed to detect EBW in the core of the QUEST. The 400 GHz gyrotron developed in the Univ. of Fukui, and the quasi-optical system will be installed on the QUEST from mid FY2019.

Kazuaki Hanada (Kyushu University) 1), 2)  
 Akira Ejiri (University of Tokyo) 3)  
 Masahiro Kobayashi (NIFS) 4)  
 Manabu Takechi (QST) 5)  
 Osamu Mitarai (Institute for Advanced Fusion  
 and Physics Education) 6)  
 Kazuo Nakamura (Kyushu University) 7)  
 Yasuhisa Oya (Shizuoka University) 8)  
 Taiichi Shikama (Kyoto University) 9)  
 Yuji Hatano (University of Toyama) 10)

Masanobu Tanaka (Pulsed Power Japan Laboratory Ltd.) 11)  
 Makoto Hasegawa (Kyushu University) 12)  
 Naoyuki Fukumoto (University of Hyogo) 13)  
 Nobuhiro Nishino (Hiroshima University) 14)  
 Masao Matsuyama (University of Toyama) 15)  
 Hiroshi Idei (Kyushu University) 16)  
 Roger Raman (University of Washington) 17)  
 Yoshihiko Hirooka (Chubu University) 18)  
 Kazuo Toi (NIFS) 19)  
 Shin Kubo (NIFS) 20)

(K.Hanada)

## University of Toyama



Arrhenius plot of permeation rates of H<sub>2</sub> and D<sub>2</sub> through Cu-0.5 mass% Al<sub>2</sub>O<sub>3</sub> oxide dispersion strengthened alloy under exposure to H<sub>2</sub> or D<sub>2</sub> mixture gas.

### Highlight

## Research Activities in Hydrogen Isotope Research Center, Organization for Promotion of Research, University of Toyama

Permeability, diffusivity and solubility of hydrogen and deuterium in Cu-0.5 mass% Al<sub>2</sub>O<sub>3</sub> oxide dispersed strengthened alloy were examined in 2018 by permeation tests using H<sub>2</sub>, D<sub>2</sub> and H<sub>2</sub>-D<sub>2</sub> mixture gases. Clear isotope effects were observed on permeability and diffusivity; the values obtained for hydrogen were larger than those for deuterium by a factor of  $\sqrt{2}$ . Namely, the difference between H and D corresponded to ratio of square root of mass.

The titles and principal investigators of research projects performed in University of Toyama in 2018 are listed below.

- (1) Isotope effects on trapping and release of hydrogen isotopes in fusion reactor materials (Y. Hatano, U. Toyama)
- (2) Hydrogen isotope transport through plasma modified fusion reactor materials (H. T. Lee, Osaka U.)
- (3) Hydrogen isotope behavior for W with controlled damage profile (Y. Oya, Shizuoka U.)
- (4) Tritium removal from tungsten by baking under deuterium gas atmosphere (Y. Nobuta, Hokkaido U.)
- (5) Tritium removal on deposited layers by glow discharge cleanings (N. Ashikawa, NIFS)
- (6) Measurement of depth distribution of hydrogen isotopes in plasma facing wall of QUEST by using GD-OES (N. Yoshida, Kyushu U.)
- (7) Tritium retention on facing materials modified by plasma wall interactions (K. Tokunaga, Kyushu U.)
- (8) Influence of impurity on the hydrogen isotope recovery performance in the plasma exhaust system (M. Kobayashi, NIFS)
- (9) The development of tritium water for inertial confinement fusion (Y. Arikawa, Osaka U.)
- (10) Gamma-ray irradiation effect on hydrogen isotopes at fusion material surfaces (T. Chikada, Shizuoka U.)
- (11) Effects of double strand break to radiation tolerance in the tardigrades (T. Miyazawa, Shizuoka U.)
- (12) Double-strand breaks in a genome-sized DNA caused by beta-ray using fluorescence microscopy (T. Kenmotsu, Doshisha U.)

The effect of microstructure on tritium transport in tungsten (W) was examined. The following results suggest tritium transport is enhanced due to the presence of grain boundaries: (1) Tritium penetration in single crystal samples was shallower in comparison to poly-crystal samples, and (2) Tritium penetration was deeper for poly-crystal samples with grains oriented perpendicular to the surface in comparison to parallel orientation.

Hydrogen isotopes retention in W with various defect distributions was evaluated. The total deuterium retention decreased with increasing damage level near the surface introduced by 3.4 MeV Fe<sup>+</sup> ion implantation. This observation indicates that the irradiation damages near the surface trap most of the deuterium and reduce the deuterium diffusion toward the bulk.

Isotope exchange in W during bake out was examined. The deuterium exposure following tritium exposure resulted in removal of ~96% of tritium. This removal extent was larger than that observed after heating in vacuum and indicates isotope exchange could enhance tritium removal.

Removal efficiencies of surface tritium on plasma facing materials by glow discharge cleaning (GDC) were investigated. Due to low sputtering yield of W by deuterium and helium, a difference between the amounts of remained tritium after GDC and initial tritium is too small. In future, operational parameters will be optimized using stainless steel samples, and then tritium removal from W will be attempted using those optimized conditions.

Behaviors of injected deuterium in several kinds of W materials were investigated by using glow-discharge optical emission spectroscopy and thermal desorption spectroscopy. In the case of hot rolled W plates, some part of the injected deuterium penetrates deeply and are strongly trapped by residual defects such as cavities.

Tritium gas exposure experiments have been carried out on high energy electron irradiated W and long term installed samples on first wall in spherical tokamak QUEST. The amount of tritium retained in surface layers of the samples has been evaluated by  $\beta$ -ray-induced X-ray spectrometry and imaging plate measurements. Tritium retention in defects/redeposition layer formed by the high energy electron irradiation/plasma-wall interactions has been discussed.

Tritium processing in the exhaust detritiation system and cryogenic isotope separation system was modeled using a simulation code. Diffusion based tritium migration in a solid with interactions to irradiation defects is applied. Gas/liquid equilibrium is a model for the isotope separation. These simulation codes will be used for the safety analysis in fusion reactor design.

Tritium doped D<sub>2</sub>O is under development for inertial confinement fusion target. In this project, T<sub>2</sub> gas is oxidized to synthesize T<sub>2</sub>O, and then it is filled (doped) into a small pellet containing D<sub>2</sub>O. In 2018, “cold run” of the system was performed by synthesizing H<sub>2</sub>O from H<sub>2</sub> and dope to D<sub>2</sub>O filled target. These results were presented as an invited talk in International Conference on Tritium Science and Technology 2019.

Deuterium depth profiles of unirradiated zirconium oxide coating samples showed a gradual decrease with depth. After gamma-ray irradiation, the deuterium concentration decreased by up to 0.1 at% with gamma-ray dose, indicating that gamma-ray irradiation reduced deuterium retention in the coatings.

Aquatic tardigrades show high radiation tolerance. The mechanisms of this tolerance are not well understood. This motivates us to investigate the effects of indirect action by gamma-rays in tardigrades (*Milnesium tardigradum*). 100 tardigrades were installed into a sample tube with a spin trap agent DMPO, and gamma-rays were irradiated up to 6000 Gy. Thereafter, electron spin resonance was applied to evaluate the quantities of radicals.

An application to measure a length of DNA before and after receiving double-strand breaks due to irradiation of beta-rays from tritium is under development by adopting analytical method of the Hough transform in image analysis of DNA taken from fluorescence microscopy observation, which is able to calculate a length of DNA more efficiently and accurately in comparison with the conventional method.

(Y. Hatano)